Zoomorphology
https://doi.org/10.1007/s00435-023-00636-1

RESEARCH

Comparative ontogeny of skin glands in *Rhinella* and *Incilius* toads

Katherine Porras-Brenes[1,2] · Nicole Ramírez-Mata[3] · Jennifer L. Stynoski[4]

Received: 27 September 2023 / Revised: 6 December 2023 / Accepted: 15 December 2023

Abstract
A key component of amphibian antipredator strategies is the chemical defenses that make them toxic and/or distasteful, like the cardiotoxic bufadienolides synthesized by the true toads and stored in granular skin glands. The morphology of adult toad glands is well-described, but the ontogenetic timing and distribution of glands during larval stages are poorly understood. A comparative understanding of granular gland development is needed to elucidate the mechanisms underlying the diversification of toad chemical defenses and their ecological roles across lineages and ontogeny. Herein, we analyzed gland morphology before and after metamorphosis of *Rhinella horribilis, Incilius melanochlorus,* and *I. luetkenii*. We hypothesized that granular gland development would begin earlier and progress faster in relatively more toxic *Rhinella* species. Our results showed that the timeline of skin development, the relative dimensions and quantity of structures, and the appearance of protein and mucin content in granular and mucous glands did not vary among *Rhinella* and *Incilius*. Furthermore, epidermal mucus and/or giant cells in larval toads may act as sources of chemical defenses prior to gland development. Our findings suggest that gland development is well-conserved among these genera; it is possible that reported differences in toxin profiles are not due to divergent morphogenesis during larval or metamorphic stages, but rather to differences in molecular function or structural differentiation in juveniles or adults. Therefore, complementary studies using integrative techniques such as immunohistochemistry and comparative transcriptomics are needed to uncover the mechanisms responsible for the diversity of chemical defenses found in bufonid toads across development.

Keywords Bufonidae · Development · Granular gland · Mucous gland · Tadpole · Morphology

Introduction

To avoid predation, amphibians rely on a diversity of antipredator strategies that include morphological and behavioral defenses (Ferreira et al. 2019; O'Donohoe et al. 2022), as well as unpalatable and/or toxic chemical defenses in skin secretions (Daly 1995; König et al. 2015; Mauricio et al. 2021). The skin of all extant amphibians contains granular glands (also known as poison, syncytial, or serous glands; Toledo and Jared 1995; Mauricio et al. 2021; O'Donohoe et al. 2022). To fill their granular glands with toxins, some anurans sequester lipophilic alkaloids from an arthropod diet (Saporito et al. 2007), and other anurans and some salamanders acquire the guanidine alkaloid tetrodotoxin thanks to symbiotic skin bacteria (Vaelli et al. 2020). However, the great majority of chemical defenses found in amphibian granular glands, such as the peptides in most anurans and the steroidal bufadienolides in the true toads (Bufonidae), are synthesized de novo by the anurans themselves (König et al. 2015).

Bufonid toads can biosynthesize an impressive diversity of bufadienolides (Rodríguez et al. 2017), which inhibit the sodium–potassium-dependent ATPase pump in cardiac membrane tissue, causing dysfunctions such as cardiac fibrosis and fatal arrhythmia (Flier et al. 1980; Deng et al. 2020). Toad skin also holds a biochemically complex cocktail of defenses including peptides, biogenic amines, indole alkaloids, lipophilic alkaloids (in the genus *Melanophryniscus*) and guanidine alkaloids (in the genus *Atelopus*; König et al.

✉ Jennifer L. Stynoski
jennifer.stynoski@ucr.ac.cr

1 Escuela de Ciencias Biológicas, Universidad Nacional, Heredia 86-3000, Costa Rica

2 Department of Biology, John Carroll University, University Heights, OH 44118, USA

3 Escuela de Biología, Universidad de Costa Rica, San José 11501-2060, Costa Rica

4 Instituto Clodomiro Picado, Universidad de Costa Rica, San José 11501-2060, Costa Rica

Published online: 19 January 2024

2015; Rodríguez et al. 2017). However, it is thought that the bufadienolides are largely responsible for the unpalatability of most developmental stages of toads to natural predators (Flier et al. 1980; Crossland 1998; Hayes et al. 2009; Stynoski and Porras-Brenes 2022). Most bufonids (over 600 species) were historically grouped into a single genus (*Bufo*), but more recently were split into several lineages including the genera *Rhinella*, *Rhaebo*, and *Incilius* that are comprised of regionally sympatric species across most of Latin America (Frost et al. 2006). The toxin profiles of toad clades, species, and even populations is highly variable (Rodríguez et al. 2017; Inoue et al. 2020), and also vary substantially across life stages (Hayes et al. 2009; Üveges et al. 2017; Ujszegi et al. 2017; Crossland et al. 2021).

Amphibian skin toxins are stored in exocrine granular glands, which are surrounded by a myoepithelial cell monolayer that contracts upon adrenergic stimulation (Toledo and Jared 1995; Nosi et al. 2002). Granular glands lack a lumen and are the only vertebrate glands that form a syncytium, which contains both the cytoplasm and secretory products of the precursor cells that break open to form it (Flucher et al. 1986). In bufonids, granular glands are dispersed across the skin surface, and in adults are aggregated in the post-ocular region where they form the prominent parotoid macroglands that are characteristic of the family (Mailho-Fontana et al. 2018). Mucous (or acinar and alveolar) glands are also dispersed across toad skin, which store mucins that keep the skin moist in terrestrial environments and provide a protective barrier in aquatic environments (Mailho-Fontana et al. 2018; Olea et al. 2019).

The structural morphology and histochemistry of toad granular glands is well described in adults (Muhse 1909; McCallion 1956; Hostetler and Cannon 1974; Cannon and Hostetler 1976; Delfino et al. 1999; Jared et al. 2009; Felsemburgh et al. 2009; Chen et al. 2017; Mailho-Fontana et al. 2020). Meanwhile, numerous studies of palatability and chemical profiles have provided evidence that some younger stages of toads are also chemically defended (Crossland 1998; Hayes et al. 2009; Llewelyn et al. 2012; Ujszegi et al. 2017; Üveges et al. 2017). A recent meta-analysis found that predators are less likely to consume young bufonid toads than young of other anuran families, presumably because they are less palatable (Stynoski and Porras-Brenes 2022). Toxin levels tend to be high in the egg and hatching stages because mother toads provision egg yolks with chemical defenses, then decrease through the larval phase until their lowest point at metamorphosis, and increase again after metamorphosis as toadlets begin biosynthesis of their own chemical defenses (Hayes et al. 2009; Llewelyn et al. 2012; Crossland et al. 2021).

Despite the apparent importance of chemical defenses in young bufonid toads, the morphological ontogeny of their skin and granular glands has only been described in three species in the genus *Rhinella* (*R. granulosa*, Chammas et al. 2014; *R. arenarum*, Regueira et al. 2016; *R. bergi*, Olea et al. 2019, also see Hayes and Gill 1995). Based on these studies, gland primordia first appear around Gosner (1960) stages 30–35, form as mucous and granular glands just before or during stages 42–44, and mature in the juvenile phase (Chammas et al. 2014; Regueira et al. 2016; Olea et al. 2019). However, it is poorly understood whether the timing and process of gland development is consistent across the family Bufonidae, including in genera besides *Rhinella*, such as *Incilius*.

Broadly in anurans, gland development commences in the epidermis with an alveolar configuration of rudimentary gland cells around pro-metamorphosis (stages 35–41). Developing glands then proliferate and migrate to the *stratus spongiosum* of the dermis for subsequent growth and differentiation, with fully formed glands containing secretory substances first appearing around metamorphosis (stages 40–44; Helff and Stark 1941; Bovbjerg 1963; Toledo and Jared 1995; Stynoski and O'Connell 2017). Gland migration is mediated by thyroid hormones and corticosterone, and thus is intricately coordinated with the initiation of metamorphosis at stage 42 (Kollros and Kaltenbach 1952; Hayes and Gill 1995). The appearance of fully formed granular glands—and in some cases partially formed glands—is also accompanied by the appearance of chemical defenses and unpalatability in various anuran families (Brodie et al. 1978; Garton and Mushinsky 1979; Stynoski et al. 2014a, b; Stynoski and O'Connell 2017; Saporito et al. 2019). Additional comparative studies of granular gland ontogeny are needed to inform our understanding of the role of developmental processes in determining the biochemical diversification and ecological roles of chemical defenses in young anurans, and in particular in the noxious bufonid toads.

In this study, we describe the developmental morphology of the skin glands of *R. horribilis* [=*marina*], *I. melanochlorus,* and *I. luetkenii,* and compare the information to that reported for *R. marina, R. granulosa,* and *R. bergi*. Specifically, to expand our understanding of the chemical defense structures of pre-metamorphic and metamorphic toads from the genera *Rhinella* and *Incilius*, we aimed to characterize the timing of granular gland development and their distribution across the skin. The toxin profiles of *Rhinella* toads are exceptionally diverse and notoriously toxic whereas *Incilius* toads are thought to specialize in the synthesis of relatively fewer and less toxic compounds like bufotenins (Rodríguez et al. 2017; Firneno et al. 2022). Hence, we hypothesized that if morphological and/or developmental differences in toxin-related structures between these genera contribute to toxin profile diversity, then integument and granular gland development would begin earlier and progress faster in *Rhinella* species than in *Incilius* species.

Methods

Study species

We collected eggs of three toad species between 2019 and 2021: *R. horribilis* and *I. luetkenii* from Guanacaste province in the North Pacific of Costa Rica (*I. luetkenii*: N 10.8767, W 85.6095; *R. horribilis*: N 10.3428, W 85.3375) and *I. melanochlorus* from Limón province in the Atlantic versant of Costa Rica (N 10.043012, W 83.540994). We can be sure of species' identities because egg strings were collected immediately following oviposition and fertilization by adult pairs of each species in field sites. *Rhinella horribilis* is distributed from southern Texas, USA to the northeastern side of the Andes mountains, although in recent years its range has expanded and it can be found in Florida, Louisiana, and some Caribbean islands (Acevedo et al. 2016). It lives up to four years, and reproduces twice a year with up to 35,000 eggs per clutch that take approximately one month to reach metamorphosis (Shanmuganathan et al. 2010). Historically, this new species was included with *R. marina*, but now the distribution range of *R. marina* is restricted geographically to the south and east of the Andes mountains (Acevedo et al. 2016). *Incilius luetkenii* is distributed along Pacific lowlands from Southern Mexico to central Costa Rica and exhibits explosive breeding after leaving subterranean burrows at the start of the rainy season (Doucet and Mennill 2010). *Incilius melanochlorus* is distributed within the wet forests of both Atlantic and Pacific lowlands in Costa Rica (O´Neill and Mendelson 2004) and reproduces in creeks and streams during the dry season (Savage 2002).

Animal rearing and preservation

We transported freshly fertilized eggs in Ziploc bags containing water from the collection sites (stream or puddle) in a chilled ice cooler to the Laboratory for the Investigation of Dangerous Animals (LIAP) at the Clodomiro Picado Institute, and reared them in similar conditions until metamorphosis. Eggs were initially left in the water in which they were collected in 10L plastic containers at ambient temperature (18–23 °C). We carefully removed grayed egg jelly as tadpoles hatched to prevent pathogen growth in the water. Once tadpoles were mobile, oriented vertically, and had visible gills (approximately stage 19), we changed 50% of the water every 1–3 days with double filtered and dechlorinated tap water, or in a few cases due to temporary issues with the filter system, with freshly collected rainwater. Once gills were absorbed (stages 23–25), we began feeding tadpoles with a mixture of tilapia food pellets and spirulina powder 2–3 times weekly. During tail reabsorption, toads were moved to small lidded plastic containers lined with very damp paper towels, and were fed tiny mealworms twice weekly.

When tadpoles reached the stages of interest, we euthanized them in a bath of 0.5% benzocaine (which produces similar histological results in young toads as euthanasia with MS-222; Regueira et al. 2016), fixed them in buffered 10% formalin for 24 h, and then stored them in 70% ethanol, changing the ethanol every 24 h for the first 72 h to remove excess formalin. In each of the three species, we preserved one to four individuals from each of four stage classes: hatchling (stages 22–25; Gosner 1960), early tadpole (stages 26–36), late tadpole (stages 37–41) and metamorph (stages 42–45), as well as one, two, three, or four weeks after metamorphosis when available due to differences in clutch size and survivorship across species (total of 66 individuals; length of individuals at each stage and species in Table S1).

Histological and staining procedure

After removing the tail and limbs, we embedded specimens in paraffin in the dorsal plane (as if these horizontally oriented animals were resting on the substrate with their ventral tissue), sectioned tissue at a thickness of 6 µm with a MICROM GmbH microtome type HM 335E (Zeiss), and mounted sections on microscope slides. We created four slides for each of the following regions of each specimen: dorsal (initial sections of paraffin block), intermediate (sections including mouthparts and digestive tissue) and ventral (later sections that no longer include mouthpart tissue).

We stained one slide per region per individual with hematoxylin and eosin (HE) to highlight general structures. Using the best-preserved section from each HE stained slide, we haphazardly selected ten points around the perimeter of the animal's body, excluding the mouth and tail, and photographed the skin tissue using a microscope (Olympus BX51) and digital camera (Olympus U-TV0.5XC-3) at 40X magnification, adding scale bars with Image Pro Express software. A preliminary analysis with eight *R. horribilis* suggested that there were no significant differences between the number or size of glands present in the anterior or posterior regions of the body across the transverse plane, so we did not discriminate between these regions when taking photos. Then, using the software ImageJ (NIH; Rasband 2012) and following the general morphometric procedure described by Chammas et al. (2014), we traced the length of the skin section within the image, and measured the thickness of the epidermis and dermis by averaging the widest, narrowest, and most intermediate thicknesses of the tissues in each image. We measured the diameters of granular and mucous glands both parallel and perpendicular to the skin surface, and calculated gland area using the formula (first

diameter/2)*(second diameter/2)*π. If there were multiple glands of each type in a given image, their area was averaged. We also counted the number of cell layers in the epidermis, the number of granular and mucous glands in the epidermis and dermis, and the number of undifferentiated glands. Mucous glands were defined as those that have a thicker membrane layer surrounding a lumen, resembling a row of bricks, whereas granular glands were considered as those surrounded only by a thin layer of myoepithelial cells, which often contained granules.

With the remaining three slides from each region of each individual (dorsal, intermediate, ventral), we stained one each with Sudan Black B to visualize lipid-based substances, Coomassie Blue R250 to visualize proteins, or Alcian Blue 8GX at pH 2.5 to visualize acidic glycoconjugates (mucopolysaccharides or mucins; Hayes and Gill 1995; Kiernan 1999; Regueira et al. 2016; O'Donohoe et al. 2022). We photographed up to five granular and five mucous glands, as available, distributed around the edge of the best-preserved section from each slide. We determined visually whether each gland showed evidence of lipid, protein, and/or mucin content within the inner membrane. We also qualitatively examined adult tissues in each species for general comparisons as well as mucus along the mouth epithelium, cranial cartilage, and hepatic tissue as positive controls for Alcian Blue, Coomassie Blue, and Sudan Black stains, respectively (not shown).

Data analysis

Developmental stages according to Gosner (1960) are not linear but rather categorical with some stages lasting longer and causing more dramatic changes in morphology than others, so we decided to group the pre-metamorphic (stage 41 or lower) and post-metamorphic (stage 42 or higher) individuals for quantitative analysis rather than including stage as a numerical predictor variable. More specific differences across stages are represented graphically.

To determine whether the area of granular and mucous glands or the thickness of the dermis or epidermis differed among the three species or pre- and post-metamorphic individuals, we used linear mixed models in the lme4 package (Bates et al. 2015) with individual as a random variable. Similarly, we used generalized linear mixed models (GLMM) with a negative binomial error distribution in the lme4 package with individual as a random variable to determine whether species or stage affected the number of granular, mucous, or undeveloped glands, or the number of cell layers in the epidermis. These quantitative analyses (granular and mucous gland number and size, epidermal and dermal thickness) were executed a second time after dividing the response variables by length of skin in the image to account for variation in skin sampling due to orientation or curvature of the tissue, but this correction did not alter any conclusions and so those results are not reported here. Furthermore, based on ANOVA and Tukey post hoc tests, the length of the skin in images of slides did not differ between species (all $p > 0.90$) or stage groups (all $p > 0.11$).

Separate mixed models were applied to determine the influence of body region (dorsal, intermediate, ventral) on granular and mucous gland area (LMM) and granular and mucous gland number (GLMM), with species as an additional fixed factor and individual as a random factor. Differences in the proportion of observed gland substances that stained with Sudan Black, Coomassie Blue, or Alcian Blue among species and stage groups were determined using GLMs with a quasibinomial error distribution due to overdispersion with binomial error distribution. When appropriate, post hoc analyses were applied using the emmeans or car packages (Fox and Weisberg 2019; Lenth 2022). All analyses were conducted in R version 4.1.2 (R Core Team 2021).

Results

Description of the ontogeny of skin and glands

A consistent pattern of skin and gland development arose in the HE slides of all three species of toads. Recently hatched tadpoles (stages 24–26; Fig. 1a) have one to two layers of epidermal cells—always a superficial (squamous or pavement) layer of triangular or cuboidal cells interspersed with abundant secretory goblet cells, and sometimes also a basal (inner) layer of larger pyramidal or columnar cells which rest on a basal lamina. Tadpoles lack evidence of both dermal development and granular or mucous glands at this stage. Melanophores could be observed just below the epidermis in the earliest stages examined and all stages thereafter. All recently hatched individuals exhibited what is known as "giant cells". These cells have also been described as Riesenzellen, clear cells, and mitochondria-rich cells (Chammas et al. 2014; Regueira et al. 2016; Fig. 2), which are only found in the basal epidermis of bufonid larvae and differ structurally and functionally from epidermal goblet cells, Leydig cells, and Kugelzellen (Fox 1988; Delfino et al. 2007). Giant cells are larger than other cells in the skin at this developmental stage (approximately 10–20 µm diameter), and may be confused with a gland as they contain secretory granules, but are comprised of a single cell with a defined nucleus that stains an intense purple color within the oval-shaped cell, which occasionally opens to the skin surface (see Fox 1988; Regueira et al. 2016). Giant cell contents in all three species stained with Alcian Blue and Coomassie Blue, but not with Sudan Black (Figs. 2 and S2).

During mid-larval development, coinciding with toe morphogenesis (stage 35; Fig. 1b; Delfino et al. 2007), the

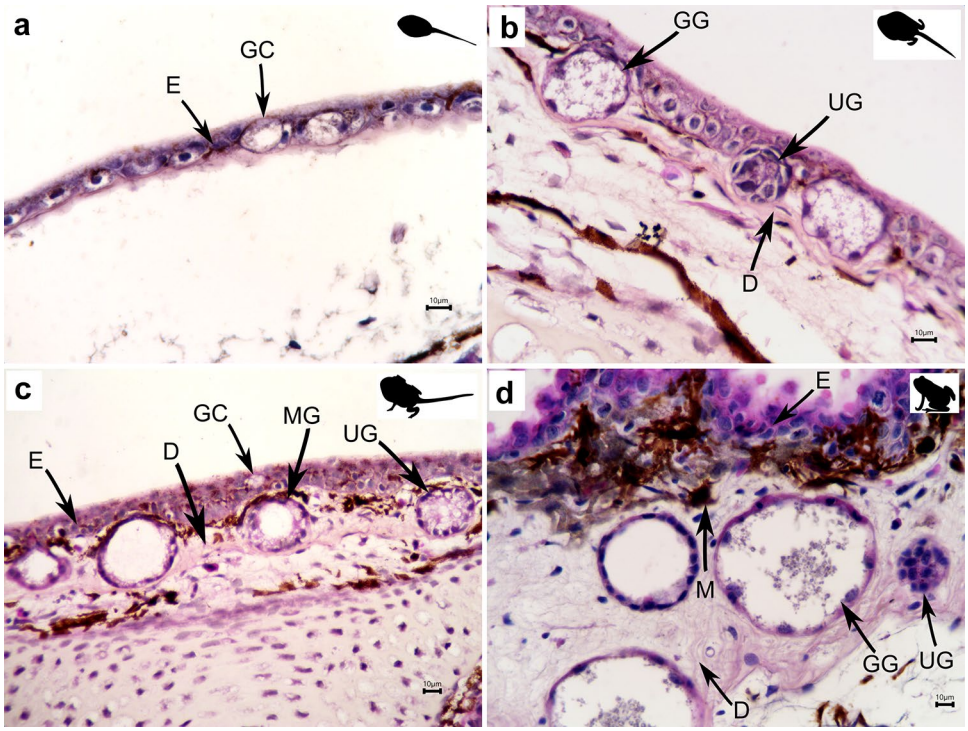

Fig. 1 Histomicrographs (40–60X) of *Rhinella horribilis* stained with Hematoxylin and Eosin at **a** recently hatched (stages 24–26), **b** pro-metamorphic (stage 40), **c** metamorphic (stage 42), and **d** post-metamorphic (1 month after stage 46) stages. *D* Dermis, *E* Epidermis, *GC* Giant Cell, *GG* Granular Gland, *M* Melanophore, *MG* Mucous Gland, *UG* Undeveloped Gland

thickness of the dermis begins to increase, and the epidermis increases from 1–2 to 2–3 layers of cells. Most individuals still exhibited giant cells, and a few also showed evidence of undeveloped glands, also known as gland nests (Hayes and Gill 1995), primordia (Toledo and Jared 1995), or Anlagen (Regueira et al. 2016). These round or oval accumulations of epidermal cells are located in the epidermis or within the intermediate layer between the epidermis and the dermis, and are distinct from the otherwise linearly aligned superficial and basal cell layers (Fig. 1b). Interestingly, one stage 35 specimen had a unicellular structure with an amoeboid form in the apical mucus of the epidermis (Figure S1). Prior to and during pro-metamorphosis which encompasses stages 35 to 41 (Fig. 1c), the dermis further thickens via division of basal cells and there is more evidence of undeveloped and now early developing glands (Fig. 3a and b). Within early granular glands, the cells expand and break open within a single-layered membrane to form a syncytium. Within early mucous glands, a circle of cuboidal secretory cells differentiates around a lumen.

During metamorphic stages 42 to 46 as well as from one week to one month after tail reabsorption, the dermis continues to thicken. The epidermis now consistently shows at least three cell layers as well as evidence of keratinization and desquamation in the outermost layer or *stratum corneum* (Fig. 1d). The epidermis also has gradually fewer goblet cells and giant cells which then are not seen after stage 42. More and larger granular and mucous glands are present and are now principally located within the dermis (Fig. 3a and b). Once in the dermis, mucous glands showed evidence of maturation (expansion, specialization of secretory cells, formation of ducts) earlier than granular glands, with mucus secretion beginning around metamorphosis. Granular content is present at these stages, but lacks structural diversity and "fullness", even one week to one month after metamorphosis (stages 42–46), compared to adult glands. Undeveloped glands lacking either lumen or syncytia were still seen in all post-metamorphic stages examined, suggesting that gland differentiation is not entirely synchronized in the skin and can still occur after metamorphosis (Fig. 1d).

There was evidence at three weeks and one month after metamorphosis of the aggregation of granular glands in the dermis parallel to the skin surface in the post-ocular region, where parotoid glands will later form. Gland ducts were seen in few sections of developing specimens of each species, but more commonly in post-metamorphic specimens (Fig. 3e). A thin layer of mucus staining with Alcian Blue was present on the exterior of the epidermis in all stages and species examined, but was more prominent in larval stages (Figs. 2a, 3a). In summary, the developmental processes and timing of morphogenetic changes associated with hatching, mid-larval, pro-metamorphic, and metamorphic stages did not differ substantially among the three species of toads examined in this study.

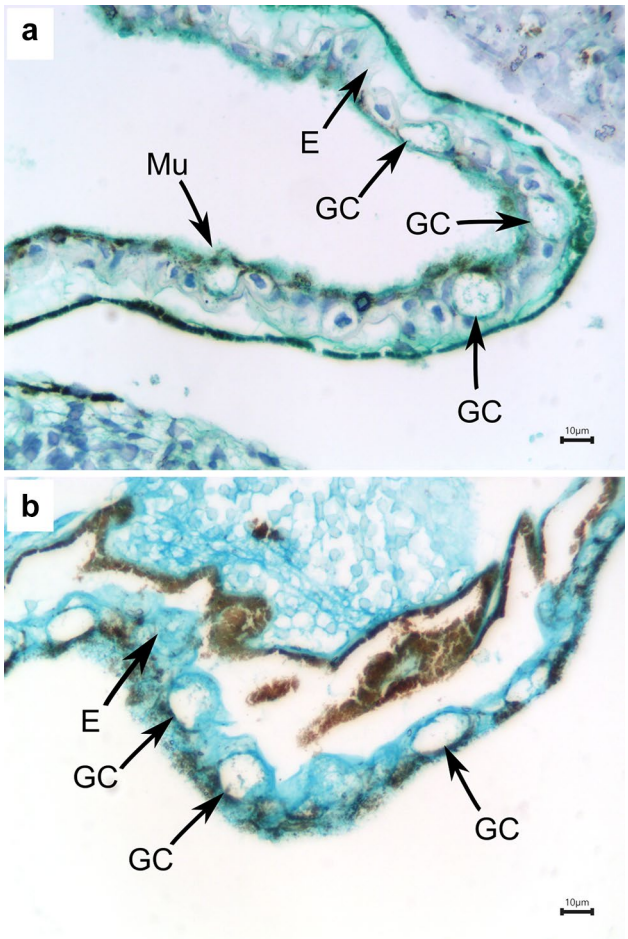

Fig. 2 Histomicrographs (60X) of giant cells in the epidermis of stage 24 *Incilius melanochlorus* stained with **a** Alcian Blue (stains mucins) and **b** Coomassie Blue (stains proteins). *E* Epidermis, *GC* Giant Cell, *Mu* Mucus layer

Quantitative analysis of skin and gland development

Granular gland area was larger in post-metamorphic toads (mean = 3947.20 $\mu m^2 \pm$ sd = 2370.41) than in pre-metamorphic toads (2558.46 ± 2130.51; $t = -3.06$, $p = 0.0004$; Figure S4). Granular gland area did not differ between *I. luetkenii* (4279.64 ± 2724.18), *I. melanochlorus* (3354.77 ± 2010.35), and *R. horribilis* (3587.04 ± 2364.27; $t = -2.12$, $p = 0.12$). Mucous gland area did not change at metamorphosis (before: 1743.92 ± 759.35, after: 2410.41 ± 1349.53; $t = -1.28$, $p = 0.13$). Mucous gland area was similar between *I. luetkenii* (2866.48 ± 1617.28), *I. melanochlorus* (2085.05 ± 1000.0), and *R. horribilis* (2269.32 ± 1261.33; $t = -1.86$, $p = 0.10$). Granular glands were typically oval shaped, as the diameter of granular glands parallel to the skin surface was longer than the diameter perpendicular to the skin surface in *I. luetkenii* (ratio of diameters X:Y: 1.45 ± 0.47), *I. melanochlorus* (1.60 ± 0.51), and *R. horribilis* (1.55 ± 0.49), whereas mucous glands were slightly more circular (*I. luetkenii*: 1.32 ± 0.36, *I. melanochlorus*: 1.54 ± 0.42, *R. horribilis*: 1.47 ± 0.40).

The number of granular glands in each image of the epidermis (uncorrected for epidermis length; see methods) was similar before (0.06 ± 0.37) and after metamorphosis (0.06 ± 0.30; $z = 0.15$, $p = 0.88$), and among the three species (*I. luetkenii*: 0.02 ± 0.16, *I. melanochlorus*: 0.07 ± 0.46, *R. horribilis*: 0.07 ± 0.34; all $p > 0.40$; Fig. 4a). The number of granular glands in the dermis increased after metamorphosis (1.61 ± 1.09) compared to before (0.19 ± 0.60; $z = -7.51$, $p < 0.0001$; Fig. 4b), but did not differ among the three species (*I. luetkenii*: 0.66 ± 1.02, *I. melanochlorus*: 0.64 ± 0.99, *R. horribilis*: 0.94 ± 1.17; all $p > 0.39$). The number of mucous glands in each image of the epidermis did not change during metamorphosis (before: 0.012 ± 0.11, after: 0.06 ± 0.30; $z = -0.03$, $p = 0.98$; Fig. 4c), and was not different among species (*I. luetkenii*: 0.02 ± 0.21, *I. melanochlorus*: 0.02 ± 0.16, *R. horribilis*: 0.04 ± 0.24; all $p > 0.92$). In the dermis, the number of mucous glands per image increased after metamorphosis (before: 0.02 ± 0.17, after: 0.78 ± 0.82; $z = -7.05$, $p < 0.0001$), but did not differ among species (*I. luetkenii*: 0.30 ± 0.69, *I. melanochlorus*: 0.24 ± 0.54, *R. horribilis*: 0.43 ± 0.71; all $p > 0.13$; Fig. 4d). The number of undeveloped glands also increased after metamorphosis (before: 0.19 ± 0.53, after: 0.60 ± 0.81; $z = -3.36$, $p = 0.0008$), but was not different among species (*I. luetkenii*: 0.32 ± 0.61, *I. melanochlorus*: 0.39 ± 0.74, *R. horribilis*: 0.37 ± 0.70; all $p > 0.64$; Figure S5). There were more granular than mucous glands at one week post-metamorphosis in all three species (granular vs. mucous; *I. luetkenii*: 1.95 ± 0.88 vs. 0.69 ± 0.73, *I. melanochlorus*: 0.95 ± 0.78 vs. 0.40 ± 0.65, *R. horribilis*: 1.76 ± 1.22 vs. 0.93 ± 0.78).

The number of cell layers in the epidermis increased from a mean of 1.74 ± 0.73 in mid-larval stages to a mean of 2.33 ± 1.40 in pro-metamorphosis ($z = 4.05$, $p < 0.0001$) and remained high at metamorphosis (2.68 ± 1.33; $z = 5.70$, $p < 0.0001$; Figure S5). The number of epidermal cell layers was higher in *I. luetkenii* (1.96 ± 0.94) than *I. melanochlorus* (1.53 ± 0.91; $z = -2.84$, $p = 0.005$), but not *R. horribilis* (2.19 ± 1.25; $z = 1.43$, $p = 0.15$). Similarly, the thickness of the epidermis increased from a mean of 25.40 µm ± 14.86 in mid-larval stages to a mean of 36.29 µm ± 26.62 in pro-metamorphosis and remained high at metamorphosis (35.78 ± 24.03; $t = 3.71$, $p = 0.0003$; Figure S5). Epidermal thickness was similar among the three species (*I. luetkenii*: 28.84 ± 22.01, *I. melanochlorus*: 31.16 ± 20.86, *R. horribilis*: 25.61 ± 14.57; all $p > 0.05$). The thickness of the dermis increased across development (all $p < 0.0001$), but did not differ

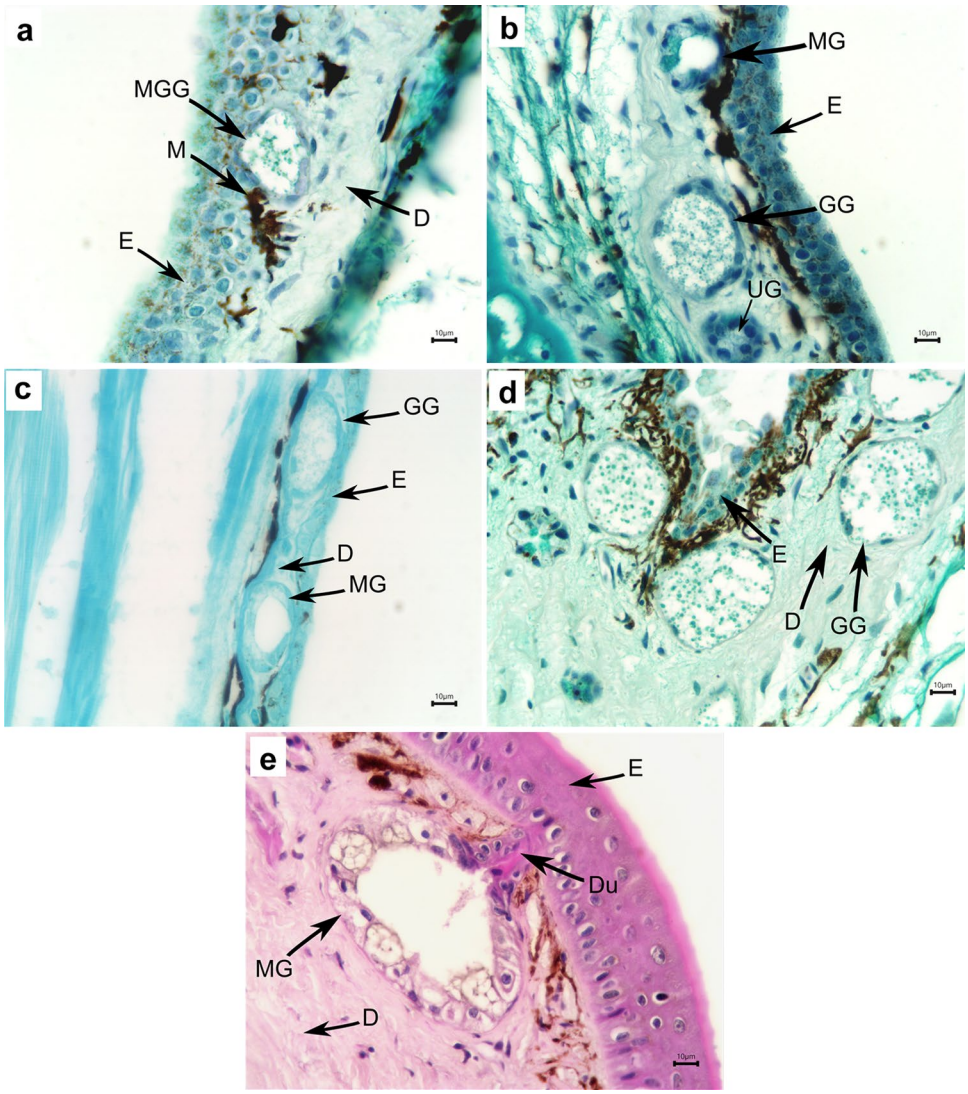

Fig. 3 Histomicrographs (40–60X) of glands in the skin of *Rhinella* and *Incilius* toads: **a** stage 40 *R. horribilis* granular gland migrating from epidermis to dermis stained positively with Alcian Blue; **b** stage 42 *R. horribilis* mucous gland, granular gland, and undeveloped gland stained positively with Alcian Blue; **c** stage 42 *R. horribilis* granular and mucous glands in the dermis stained positively with Coomassie Blue; **d** two weeks after stage 46 *R. horribilis* with two undeveloped but likely mucous glands and four granular glands in the dermis stained positively with Alcian Blue; **e** adult *I. luetkenii* mucous gland in the dermis with a duct through the epidermis stained with Hematoxylin and Eosin. *D* Dermis, *Du* Duct, *E* Epidermis, *GG* Granular Gland, *M* Melanophore, *MG* Mucous Gland, *MGG* Migrating Granular Gland, *UG* Undeveloped Gland

significantly between *I. luetkenii* (34.49 ± 41.88), *I. melanochlorus* (32.95 ± 41.88), and *R. horribilis* (36.27 ± 35.30; $t = -1.67$, $p = 0.24$ Figure S5).

Granular glands were larger in the dorsal region (4095.39 $\mu m^2 \pm 2648.26$) than in the intermediate (3536.55 ± 2235.67) or ventral (3356.00 ± 2151.81) regions ($t = -2.08$, $p = 0.003$), but did not differ by species ($t = -0.97$, $p = 0.16$). Also, there were more granular glands per image from the dorsal region (0.94 ± 1.19) than in the ventral region (0.70 ± 1.04; $z = -2.24$, $p = 0.025$), and this difference was consistent across all three species ($z = 1.73$, $p = 0.08$). On the other hand, mucous glands had a similar area across body regions (dorsal: 2521.43 $\mu m^2 \pm 1432.53$, intermediate: 2205.92 ± 1097.51, ventral: 2354.11 ± 1409.56; $t = -1.91$, $p = 0.09$) and species ($t = -2.06$, $p = 0.07$). The number of mucous glands did not differ among body regions (dorsal: 0.36 ± 0.65, intermediate: 0.35 ± 0.65, ventral: 0.40 ± 0.76; $z = 0.73$, $p = 0.46$) or species ($z = 0.34$, $p = 0.73$).

Histochemistry

Among the 38 individuals in which glands were detected, the proportion of granular and mucous glands with contents that stained with Alcian Blue was close to 1.0 and did not differ among stages (granular: all $p > 0.99$, mucous: all $p > 0.09$) or species (granular: all $p > 0.99$, mucous: all $p > 0.55$). Similarly, the proportion of granular glands with contents that stained with Coomassie Blue was close to 1.0 in most images and did not differ among stages (all $p > 0.99$) or species (all $p > 0.99$). The proportion of mucous glands that stained with Coomassie Blue was more heterogeneous than with Alcian Blue with fewer individual mucous glands staining positively for Coomassie Blue, but in spite of this higher variability, differences among species and stages were still not statistically significant (stages: all $p > 0.99$, species: all $p > 0.45$). We did not detect Sudan Black B staining

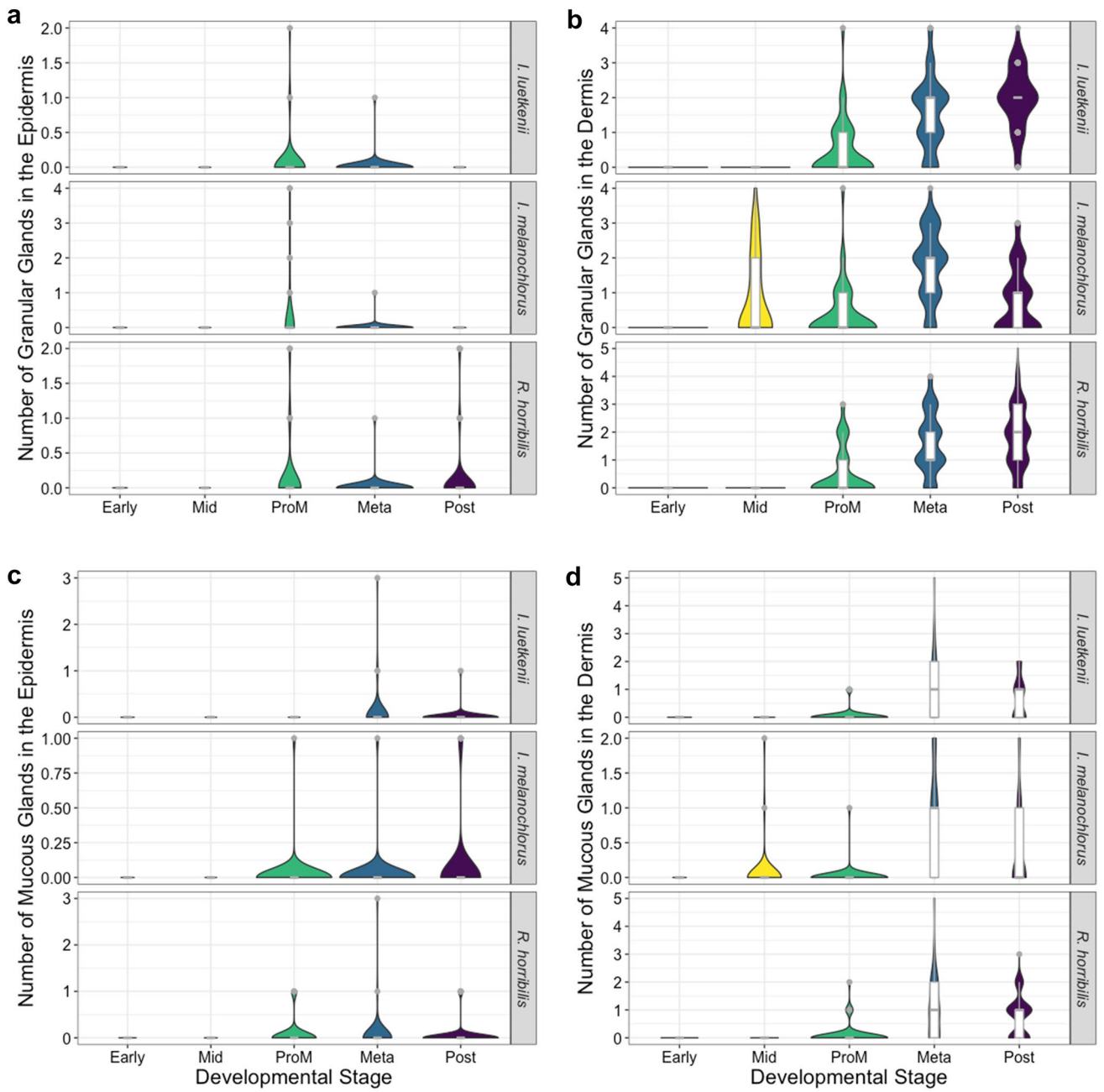

Fig. 4 The number of granular (**a**, **b**) and mucous (**c**, **d**) glands present in each of 10 images per individual of epidermal (**a**, **c**) and dermal (**b**, **d**) skin layers during development in three species of toads. Mid-larval stages (Mid) are represented in yellow, pro-metamorphic (ProM) stages in green, metamorphic (Meta) stages in blue, and post-metamorphic (Post) stages in purple. Violin plots showing overall distribution of data points are overlayed with boxplots. Flat lines represent individuals with zero glands

within gland membranes or contents in any of the glands examined in any species or stage of development (see below, Figure S3).

Discussion

The origin of diversity of chemical defenses in different species and life stages of bufonid toads is not well understood (Rodríguez et al. 2017; Inoue et al. 2020; Crossland et al. 2021). We compared the morphometric development of the integument and secretory glands among *Rhinella* and *Incilius* toads, and found that both qualitatively and

quantitatively the patterns of development of the epidermis, dermis, glands, and secretory products were similar across the three species examined in this study and three previously examined *Rhinella* species (Chammas et al. 2014; Regueira et al. 2016; Olea et al. 2019; Table S2). Therefore, our findings suggest that skin ontogeny in the family Bufonidae is well conserved. Differences among toad stages and lineages in toxin profiles might be due to differences in molecular function (i.e., gene sequences, gene expression, or protein translation and folding) or perhaps to structural differentiation later in juvenile or adult stages rather than during larval or metamorphic stages (see Regueira et al. 2017).

Early in development (*i.e.,* pre- and pro-metamorphic stages), toads do not appear to have granular glands capable of producing or storing toxic or unpalatable substances for defense against predators and pathogens (Hayes et al. 2009). In *R. marina,* eggs are endowed with maternal toxins, and, accordingly, bufadienolide profiles of eggs are very similar to the profiles of adult parotoid glands (Hayes et al. 2009; Crossland et al. 2021; but see Üveges et al. 2017). After metamorphosis, granular glands mature and then begin to fill with substances that differ chemically from adult bufadienolides but are nonetheless unpalatable and/or toxic (Freeland and Kerin 1991; Hayes et al. 2009; Crossland et al. 2021). The larval period between the post-hatching loss of maternally provisioned toxins and the post-metamorphic self-production of toxins may represent a vulnerable phase, a pattern supported by numerous studies of the palatability of toad tadpoles (Brodie et al. 1978; Crossland 1998; Stynoski and Porras-Brenes 2022). However, toad larvae may be capable of synthesizing chemical defenses in tissues other than the skin glands (Üveges et al. 2017; Sun et al. 2022), which may explain why the relative abundance of some steroid compounds (i.e., bufagenins versus bufotoxins, respectively) are distinct between young and adult toads (Ujszegi et al. 2017; Crossland et al. 2021). Also, other chemical defenses may be present in the mucus that lines the exterior of the epidermis or within the abundant giant cells of toad larvae who do not yet possess mature granular glands (Regueira et al. 2016). However, more work is needed to determine the identity and defensive function of such substances and their degree of toxicity and/or unpalatability (see Raices et al. 2020).

We identified an abundance of giant cells in stages 24–42 of all three species, which are an epidermal structure unique to larval bufonid toads (Delfino et al. 2007). Giant cells contain secretory granules that are visually similar to the granules in mature granular glands and are thought to function in mucosal hydration and in storage of peptide-based alarm cues such as suberic acid (Delfino et al. 2007; Regueira et al. 2016; Crossland et al. 2019; Raices et al. 2020; Jungblut et al. 2022). Numerous anurans, particularly those displaying schooling behavior, have been reported to perform a "flight reaction" or other behavioral shifts upon exposure to broken skin tissue of toad tadpoles, presumably to avoid impending predation risk (Fraker et al. 2009; Crossland et al. 2019). Recent work demonstrated that *R. arenarum* tadpoles rapidly increased activity levels in response to macerated conspecific tadpole homogenates, but only after the macerated tadpoles had reached stage 22 (Jungblut et al. 2022). In accordance with this behavior, giant cells first appear at stage 22 in *R. arenarum* (Jungblut et al. 2022) and *B. bufo* (Fox 1988). We also identified these cells in *R. horribilis*, *I. luetkenii*, and *I. melanochlorus* from stages 24–26 up to stage 42, and histochemical staining indicated that they contain mucins and proteins, but not lipids, similar to reports in *R. arenarum* (Regueira et al. 2016). Thus, giant cells and their protein-based contents may play an important role in the antipredator strategy of young toads by allowing them to communicate via alarm cues prior to the development of mature granular glands.

In contrast to the granular glands, the mucous glands are more mature and producing secretions before metamorphosis, as in other species (Regueira et al. 2016). In adult anurans, mucous glands are smaller than granular glands, which accordingly take longer to develop (Toledo and Jared 1995; Chammas et al. 2014). Furthermore, we found that while mucous glands had a similar size and density in the ventral and dorsal regions of the body, there were more granular glands and larger granular glands in the dorsal region. A few other studies have also identified larger and/or higher density of granular glands in the dorsal region in metamorphic toads (*R. bergi,* Olea et al. 2019; *R. ornata,* Felsemburgh et al. 2009; *Anaxyrus americanus* McCallion 1956; but see Chammas et al. 2014 about *R. granulosa*). The distribution of developing granular glands could reflect the terrestrial lifestyle of juvenile and adult toads, which are mostly exposed to predators via the dorsum. Conversely, anurans with a mostly aquatic lifestyle tend to have glands that are evenly distributed across the body, given that their predators can attack from many angles (Garton and Mushinsky 1979). Thus, the relative density, size, and location of glands may each play a role in the degree of hydration, toxicity, and/or unpalatability of different species and life stages of anurans, in response to the context of their specific predator, disease, and desiccation risks (Toledo and Jared 1995; Saporito et al. 2010; Regueira et al. 2017).

We did not find clear evidence of Sudan Black B staining in the glands of any specimens, including in *R. horribilis* one month after metamorphosis (approximately 10 mm snout-vent length or SVL). In a closely related species, *R. marina*, juveniles with a 24–25 mm SVL display a red–orange pigmentation on their recently formed parotoid glands, and relative parotoid dry weight and volume increases dramatically both at 24 mm and again at 70 mm (Freeland and Kerin 1991). Similarly, granular gland contents of *R. arenarum* juveniles first showed lipidic histochemical reactions at

50 mm (Regueira et al. 2017). Thus, it may well be that toads at the developmental stages that were examined in the current study do not yet synthesize or store lipid- or cholesterol-based toxins in their glands or macroglands (as in *R. arenarum*; Regueira et al. 2016). Although parotoid glands containing secretory products were distinguishable in histological sections three and four weeks after metamorphosis and have been reported at 18–29 days post-metamorphosis in other bufonids (Licht 1967; Chammas et al. 2014; Regueira et al. 2016; Olea et al. 2019), those products could be comprised of substances other than cardiotonic steroids until completion of gland maturation during the juvenile phase (Chammas et al. 2014; Regueira et al. 2017).

Lipid stains have not reacted with granular contents in various studies of recently metamorphosed toads (Regueira et al. 2016 with Sudan Red III, Olea et al. 2019 with Oil Red, current study), even though Sudan Black B has reacted with the lipidic contents of adult granular glands following preservation in formaldehyde-based solutions in several species (*Xenopus laevis,* Hayes and Gill 1995; *Clinotarsus curtipes*, Gosavi et al. 2014; *R. marina,* Mailho-Fontana et al. 2018; *Odontophrynus occidentalis*, O'Donohoe et al. 2022). A lack of lipid staining in young toads might indicate that developing individuals are not yet producing or storing significant quantities of steroid toxins in their glands. However, some other studies—including studies with adult bufonids—have also failed to show conclusive lipid staining of granular gland content (*R. marina*, Hostetler and Cannon 1974; *I. alvarius,* Cannon and Hostetler 1976; *Anaxyrus boreas* Hayes and Gill 1995), which calls into question whether lipid staining following formaldehyde-based preservation is the ideal way to detect and visualize bufadienolides in toad skin glands in future histochemical studies. Lipid staining of granular glands in numerous non-bufonid families also highlights the well-known fact that these staining methods are not specific to bufadienolides (which are unique to toads), but rather stain many types of lipids and steroids.

Current knowledge of the presumed localization of bufadienolide synthesis and storage is based on classic histochemistry, but new techniques such as DESI-MSI visualization (Mailho-Fontana et al. 2020; Sun et al. 2022), steroid labeling, and mRNA-based immunohistochemistry of candidate enzymes (for example, CYP2s) in bufadienolide biosynthesis pathways (Sciani et al. 2019; Sun et al. 2022; Firneno et al. 2022; Lv et al. 2022) are likely to provide fresh insights. For example, using DESI-MSI in stage 42 *Bufo gargarizans*, Sun et al. (2022) found evidence that bufadienolides may, in fact, be produced and stored in the liver and gallbladder of tadpoles rather than in the myoepithelial cells of the skin (Mailho-Fontana et al. 2020; see also Firneno et al. 2022). Together, these findings open up the possibility that granular skin glands in toads may function primarily in storage rather than in biosynthesis, much as in the closely related Dendrobatidae, which store lipophilic alkaloids derived from an arthropod diet in their granular skin glands (Saporito et al. 2010, 2019; Stynoski and O'Connell 2017).

The bufonid toads have benefited enormously from the chemical defenses in their specialized integumentary structures. Their toxins have allowed some species to invade many areas globally (Sales et al. 2021). Distinct components of their chemical defenses have likely contributed to the fact that some toad lineages such as *Rhinella* and *Incilius* are resistant to recent population declines of many amphibians, whereas other toad lineages such as *Atelopus* are particularly vulnerable to the same anthropogenic and pathogenic threats, especially in the larval phase (Catenazzi et al. 2018; Scheele et al. 2019). Overall, the family Bufonidae can synthesize an impressive diversity of chemical defenses, but the mechanisms that underlie the synthesis, storage, and delivery of the majority of those substances remain a mystery. In this study, we aimed to understand whether differences in the structural development of the skin and glands could be associated with differences in the general chemical profiles that have been described in two genera of bufonid toads. However, our results instead provide evidence that the ontogeny of integumentary structures is well conserved across the genera *Rhinella* and *Incilius* and, therefore, we speculate that differences in chemical profiles are likely the result of distinct molecular processes in the two lineages.

Supplementary Information The online version contains supplementary material available at https://doi.org/10.1007/s00435-023-00636-1.

Acknowledgements We thank Mahmood Sasa, Fabián Bonilla, Sofía Granados-Martínez, Davinia Beneyto, Felipe Triana R., Carolina Esquivel D., Randall Jiménez Q., and María Marta Chavarría for their assistance with field work, sample processing, and analysis. Funding was provided by the Vicerrectoría de Investigación of the University of Costa Rica (Fondo Semilla 741-C0-470 to JLS) and the International Centre for Genetic Engineering and Biotechnology (ICGEB Early Career CRP/CPI19-04 to JLS).

Author contributions KPB and JLS conceived the study and wrote the manuscript. JLS analyzed the data. All authors contributed to the collection of data and manuscript editing and approval.

Funding Funding was provided by the Vicerrectoría de Investigación of the University of Costa Rica (Fondo Semilla 741-C0-470 to JLS) and the International Centre for Genetic Engineering and Biotechnology (ICGEB Early Career CRP/CPI19-04 to JLS). Funding sponsors did not play any role in study design, in the collection, analysis and interpretation of the data, in the writing of the report, or in the decision to submit the article for publication.

Data and code availability All data generated or analyzed during this study are available from the corresponding author upon reasonable request.

Declarations

Conflict of interest The authors have no competing interests to declare that are relevant to the content of this article.

Ethical approval All procedures in this experiment were approved by the Institutional Animal Care and Use Committee of the University of Costa Rica (UCR; CICUA-020–2019), as well as the Biodiversity Committee of the UCR (Resolución 218) and the Sistema Nacional de Áreas de Conservación of the Ministerio del Ambiente y Energía de Costa Rica (SINAC; M-P-SINAC-PNI-ACAT-050–2019, R-SINAC-ACG-PI-002–2020, R-SINAC-PNI-ACLAC-048–2019).

References

Acevedo AA, Lampo M, Cipriani R (2016) The cane or marine toad, *Rhinella marina* (Anura, Bufonidae): two genetically and morphologically distinct species. Zootaxa 4103:574–586

Bates D, Mächler M, Bolker B, Walker S (2015) Fitting linear mixed-effects models using lme4. J Stat Softw 67:1–48

Bovbjerg AM (1963) Development of the glands of the dermal plicae in *Rana pipiens*. J Morphol 113:231–243

Brodie ED, Formanowicz DR, Brodie ED (1978) The development of noxiousness of *Bufo americanus* tadpoles to aquatic insect predators. Herpetologica 34:302–306

Cannon MS, Hostetler JR (1976) The anatomy of the parotoid gland in *Bufonidae* with some histochemical findings II. Bufo Alvarius. J Morphol 148:137–159

Catenazzi A, Flechas SV, Burkart D, Hooven ND, Townsend J, Vredenburg VT (2018) Widespread elevational occurrence of antifungal bacteria in Andean amphibians decimated by disease: a complex role for skin symbionts in defense against chytridiomycosis. Front Microbiol 9:1–14

Chammas SM, Carneiro SM, Ferro RS, Antoniazzi MM, Jared C (2014) Development of integument and cutaneous glands in larval, juvenile and adult toads (*Rhinella granulosa*): a morphological and morphometric study. Acta Zool 96:460–477

Chen W, Hudson CM, DeVore JL, Shine R (2017) Sex and weaponry: the distribution of toxin-storage glands on the bodies of male and female cane toads (*Rhinella marina*). Ecol Evol 7:8950–8957

Crossland MR (1998) Ontogenetic variation in toxicity of tadpoles of the introduced toad *Bufo marinus* to native Australian aquatic invertebrate predators. Herpetologica 54:364–369

Crossland MR, Salim AA, Capon RJ, Shine R (2019) The effects of conspecific alarm cues on larval cane toads (*Rhinella marina*). J Chem Ecol 45:838–848

Crossland MR, Salim AA, Capon RJ, Shine R (2021) Chemical cues that attract cannibalistic cane toad (*Rhinella marina*) larvae to vulnerable embryos. Sci Rep 11:12527

Daly JW (1995) The chemistry of poisons in amphibian skin. Proc Nat Acad Sci USA 92:9–13

Delfino G, Brizzi R, Alvarez BB, Taddei L (1999) Secretory polymorphism and serous cutaneous gland heterogeneity in *Bufo granulosus* (Amphibia, Anura). Toxicon 37:1281–1296

Delfino G, Quagliata S, Giachi F, Malentacchi C (2007) Kugelzellen in larval anuran epidermis: An ultrastructural study on tadpoles of *Pelobates cultripes* (Pelobatidae) and *Phyllobates bicolor* (Dendrobatidae). Contrib to Zool 76:213–220

Deng LJ, Li Y, Qi M et al (2020) Molecular mechanisms of bufadienolides and their novel strategies for cancer treatment. Eur J Pharmacol 887:173379

Doucet SM, Mennill DJ (2010) Dynamic sexual dichromatism in an explosively breeding neotropical toad. Biol Lett 6:63–66

Felsemburgh FA, de Almeida PG, de Carvalho-E-Silva SP, de Brito-Gitirana L (2009) Microscopical methods promote the understanding of the integument biology of *Rhinella ornata*. Micron 40:198–205

Ferreira RB, Lourenço-de-Moraes R, Zocca C, Duca C, Beard KH, Brodie ED (2019) Antipredator mechanisms of post-metamorphic anurans: a global database and classification system. Behav Ecol Sociobiol 73:1–21

Firneno TJ, Ramesh B, Maldonado JA et al (2022) Transcriptomic analysis reveals potential candidate pathways and genes involved in toxin biosynthesis in true toads. J Hered 113:311–324

Flier J, Edwards MW, Daly JW, Myers CW (1980) Widespread occurrence in frogs and toads of skin compounds interacting with the ouabain site of Na+, K+-ATPase. Science 208:503–505

Flucher BE, Lenglachner-Bachinger C, Pohlhammer K, Adam H, Mollay C (1986) Skin peptides in *Xenopus laevis*: Morphological requirements for precursor processing in developing and regenerating granular skin glands. J Cell Biol 103:2299–2309

Fox H (1988) Riesenzellen, goblet cells, leydig cells and the large clear cells of *Xenopus*, in the amphibian larval epidermis: fine structure and a consideration of their homology. J Submicrosc Cytol Pathol 20:437–451

Fox J, Weisberg S (2019) An {R} Companion to applied regression, Third Edition. Thousand Oaks CA: Sage. URL: https://socialsciences.mcmaster.ca/jfox/Books/Companion/

Fraker ME, Hu F, Cuddapah V, McCollum SA, Relyea RA, Hempel J, Denver RJ (2009) Characterization of an alarm pheromone secreted by amphibian tadpoles that induces behavioral inhibition and suppression of the neuroendocrine stress axis. Horm Behav 55:520–529

Freeland WJ, Kerin SH (1991) Ontogenetic alteration of activity and habitat selection by *Bufo marinus*. Wildl Res 18:431–443

Frost DR, Grant T, Faivovich J et al (2006) The amphibian tree of life. Bull Am Mus Nat Hist 2006:1–291

Garton JD, Mushinsky HR (1979) Integumentary toxicity and unpalatability as an antipredator mechanism in the narrow mouthed toad, *Gastrophryne carolinensis*. Can J Zool 57:1965–1973

Gosavi SM, Gaikwad PS, Gramapurohit NP, Kumar AR (2014) Occurrence of parotoid glands in tadpoles of the tropical frog, *Clinotarsus curtipes* and their role in predator deterrence. Comp Biochem Physiol Part A Mol Integr Physiol 170:31–37

Gosner KL (1960) A simplified table for staging anuran embryos and larvae with notes on identification. Herpetologica 16:183–190

Hayes TB, Gill TN (1995) Hormonal regulation of skin gland development in the toad (*Bufo boreas*): the role of the thyroid hormones and corticosterone. Gen Comp Endocrinol 99:161–168

Hayes RA, Crossland MR, Hagman M, Capon RJ, Shine R (2009) Ontogenetic variation in the chemical defenses of cane toads (*Bufo marinus*): toxin profiles and effects on predators. J Chem Ecol 35:391–399

Helff OM, Stark W (1941) Studies on amphibian metamorphosis XVIII. The development of structures in the dermal plicae of *Rana sylvatica*. J Morphol 68:303–329

Hostetler JR, Cannon MS (1974) The anatomy of the parotoid gland in *Bufonidae* with some histochemical findings. I Bufo Marinus J Morphol 142:225–239

Inoue T, Nakata R, Savitzky AH, Yoshinaga N, Mori A, Mori N (2020) Variation in bufadienolide composition of parotoid gland secretion from three taxa of Japanese toads. J Chem Ecol 46:997–1009

Jared C, Antoniazzi MM, Jordão AE, Silva JRM, Greven H, Rodrigues MT (2009) Parotoid macroglands in toad (*Rhinella jimi*): their structure and functioning in passive defence. Toxicon 54:197–207

Jungblut LD, Raices M, Rincón-Camacho L, Pozzi AG (2022) Co-occurrence between the presence of epidermal giant cells and alarm chemical cues in tadpole skin homogenates: an ontogenetic and cross-species comparison analysis. Zoology 153:126024

Kiernan JA (1999) Histological and histochemical methods: theory and practice, 3rd edn. Butterworth-Heinemann, Oxford, UK

Kollros JJ, Kaltenbach JC (1952) Local metamorphosis of larval skin in *Rana pipiens*. Physiol Zool 25:163–170

König E, Bininda-Emonds OR, Shaw C (2015) The diversity and evolution of anuran skin peptides. Peptides 63:96–117
Lenth RV (2022) Emmeans: estimated marginal means, aka least-squares means. R package version 1.7.4–1. https://CRAN.R-project.org/package=emmeans
Licht LE (1967) Initial appearance of the parotoid gland in three species of toads (genus *Bufo*). Herpetologica 23:115–118
Llewelyn J, Bell K, Schwarzkopf L, Alford RA, Shine R (2012) Ontogenetic shifts in a prey's chemical defences influence feeding responses of a snake predator. Oecologia 169:965–973
Lv Y, Li Y, Wen Z, Shi Q (2022) Transcriptomic and gene-family dynamic analyses reveal gene expression pattern and evolution in toxin-producing tissues of Asiatic toad (*Bufo gargarizans*). Front Ecol Evol 10:745
Mailho-Fontana PL, Antoniazzi MM, Sciani JM, Pimenta DC, Barbaro KC, Jared C (2018) Morphological and biochemical characterization of the cutaneous poison glands in toads (*Rhinella marina* group) from different environments. Front Zool 15:1–15
Mailho-Fontana PL, Porcari AM, Eberlin MN et al (2020) Distribution of major toxins in *Rhinella marina* parotoid macroglands using desorption-electrospray-ionization mass spectrometry imaging (DESI-MSI). Toxicon X 6:100033
Mauricio B, Mailho-Fontana PL, Sato LA et al (2021) Morphology of the cutaneous poison and mucous glands in amphibians with particular emphasis on caecilians (*Siphonops annulatus*). Toxins 13:779
McCallion DJ (1956) The parotoid gland of the toad, *Bufo americanus*. Can J Zool 34:174–177
Muhse EF (1909) The cutaneous glands of the common toads. Am J Anat 9:321–359
Nosi D, Terreni A, Alvarez B, Delfino G (2002) Serous gland polymorphism in the skin of *Phyllomedusa hypochondrialis azurea* (Anura, Hylidae): response by different gland types to norepinephrine stimulation. Zoomorphology 121:139–148
O'Neill EM, Mendelson JR (2004) Taxonomy of Costa Rican toads referred to *Bufo melanochlorus* cope, with the description of a new species. J Herpetol 38:487–494
O'Donohoe MA, Rosset SD, Regueira E, Haddad CF, Basso NG, Hermida GN (2022) Comparative skin histology of neotropical odontophrynid frogs. Zool Anz 301:127–144
Olea GB, Cheij EO, Curi LM, Boccioni APC, Céspedez JA, Lombardo DM (2019) Histological and immunohistochemical characterization of the integument and parotoids glands *Rhinella bergi* (Anura: Bufonidae): Development and differentiation. Acta Histochem 121:277–283
R Core Team (2021) R: a language and environment for statistical computing. R Foundation for Statistical Computing, Vienna, Austria. URL https://www.R-project.org/
Raices M, Jungblut LD, Pozzi AG (2020) Evidence of the peptide identity of the epidermal alarm cue in tadpoles of the toad *Rhinella arenarum*. Herpetol J 30:230–233
Rasband WS (2012) ImageJ: Image processing and analysis in Java. Astrophys Sour Code Libr. ascl-1206
Regueira E, Dávila C, Hermida GN (2016) Morphological changes in skin glands during development in *Rhinella arenarum* (Anura: Bufonidae). Anat Rec 299:141–156
Regueira E, Dávila C, Sassone AG, O'Donohoe MEA, Hermida GN (2017) Post-metamorphic development of skin glands in a true toad: parotoids versus dorsal skin. J Morphol 278:652–664
Rodríguez C, Rollins-Smith L, Ibáñez R, Durant-Archibold AA, Gutiérrez M (2017) Toxins and pharmacologically active compounds from species of the family *Bufonidae* (Amphibia, Anura). J Ethnopharmacol 198:235–254
Sales LP, Rebouças R, Toledo LF (2021) Native range climate is insufficient to predict anuran invasive potential. Biol Invasions 23:2635–2647
Saporito RA, Donnelly MA, Norton RA, Garraffo HM, Spande TF, Daly JW (2007) Oribatid mites as a major dietary source for alkaloids in poison frogs. Proc Nat Acad Sci USA 104:8885–8890
Saporito RA, Isola M, Maccachero VC, Condon K, Donnelly MA (2010) Ontogenetic scaling of poison glands in a dendrobatid poison frog. J Zool 282:238–245
Saporito RA, Russell MW, Richards-Zawacki CL, Dugas MB (2019) Experimental evidence for maternal provisioning of alkaloid defenses in a dendrobatid frog. Toxicon 161:40–43
Savage JM (2002) The amphibians and reptiles of Costa Rica. The University of Chicago Press, p 934
Scheele BC, Pasmans F, Skerratt LF et al (2019) Amphibian fungal panzootic causes catastrophic and ongoing loss of biodiversity. Science 363:1459–1463
Sciani JM, Neves A, Vassão RC, Spencer P, Antoniazzi MM, Jared C, Pimenta DC (2019) The amphibian diacylglycerol O-acyltransferase 2 (DGAT2): a 'paleo-protein'with conserved function but unique folding. Prot J 38:83–94
Shanmuganathan T, Pallister J, Doody S et al (2010) Biological control of the cane toad in Australia: a review. Anim Conserv 13:16–23
Stynoski JL, O'Connell LA (2017) Developmental morphology of granular skin glands in pre-metamorphic egg-eating poison frogs. Zoomorphology 136:219–224
Stynoski JL, Porras-Brenes K (2022) Meta-analysis of tadpole taste tests: consumption of anuran prey across development and predator strategies. Oecologia 199:845–857
Stynoski JL, Torres-Mendoza Y, Sasa-Marin M, Saporito RA (2014a) Evidence of maternal provisioning of alkaloid-based chemical defenses in the strawberry poison frog *Oophaga pumilio*. Ecology 95:587–593
Stynoski JL, Shelton G, Stynoski P (2014b) Maternally derived chemical defences are an effective deterrent against some predators of poison frog tadpoles (*Oophaga pumilio*). Biol Lett 10:20140187
Sun B, Jiang S, Li M et al (2022) Lipidomics combined with transcriptomic and mass spectrometry imaging analysis of the Asiatic toad (*Bufo gargarizans*) during metamorphosis and bufadienolide accumulation. Chinese Med 17:123
Toledo RD, Jared C (1995) Cutaneous granular glands and amphibian venoms. Comp Biochem Physiol Part A Physiol 111:1–29
Ujszegi J, Móricz ÁM, Krüzselyi D, Hettyey A (2017) Skin toxin production of toads changes during early ontogeny but is not adjusted to the microbiota of the aquatic environment. Evol Ecol 31:925–936
Üveges B, Fera G, Móricz ÁM, Krüzselyi D, Bókony V, Hettyey A (2017) Age-and environment-dependent changes in chemical defences of larval and post-metamorphic toads. BMC Evol Biol 17:1–10
Vaelli PM, Theis KR, Williams JE, O'Connell LA, Foster JA, Eisthen HL (2020) The skin microbiome facilitates adaptive tetrodotoxin production in poisonous newts. Elife 9:e53898